Invited paper presented at the ENAM'95 Conference
(Exotic Nuclei & Atomic Masses), Arles, June 19–23

TRI–PP–95–56
August 1995

THE β-DELAYED α-SPECTRUM OF ^{16}N AND THE ASTROPHYSICAL ASPECTS OF THE ^{12}C(α,γ)^{16}O REACTION

R.E. Azuma[1], L. Buchmann[2], F.C. Barker[3], C.A. Barnes[4], J.M. D'Auria[5], M. Dombsky[5,6], U. Giesen[1,2], K.P. Jackson[2,5], J. Humblet[4,7], J.D. King[1], R.G. Korteling[5], K. Langanke[4], P. McNeely[6], J. Powell[1], G. Roy[6], J. Vincent[2], T.R. Wang[1,4], S.S.M. Wong[1], and P.R. Wrean[4]

[1]*Department of Physics, University of Toronto, Toronto, Ontario, Canada M5S 1A7*
[2]*TRIUMF, 4004 Wesbrook Mall, Vancouver, B.C., Canada V6T 2A3*
[3]*Department of Physics, Australian National University, Canberra, A.C.T. 0200, Australia*
[4]*W.K. Kellogg Laboratory, California Institute of Technology, Pasadena, CA 91125*
[5]*Department of Chemistry, Simon Fraser University, Burnaby, B.C., Canada V5A 1S6*
[6]*Department of Physics, University of Alberta, Edmonton, Alberta, Canada T6G 2J1*
[7]*Institut de Physique, Université de Liege, Liege, Belgium*

(June, 1995)

Abstract

Radiative alpha-capture by ^{12}C is a key process occurring during the helium-burning phase in red giant stars, and its rate remains one of the most significant uncertainties in the nucleosynthetic calculations for massive stars. This is largely due to the lack of precise experimental information concerning the values of the reduced α-particle widths of the $J^\pi=1^-$ and 2^+ subthreshold states in ^{16}O to which the higher-energy radiative capture data are only weakly sensitive. Of these two states, the reduced α-width of the $E_x=7.12$ MeV $J^\pi=1^-$ level has been predicted to have a considerable effect on the structure of the hitherto unmeasured low-energy region of the β-delayed α-particle spectrum of ^{16}N. Experiments using the TRIUMF isotope separator TISOL have been performed to measure this α-spectrum down to an energy of $E_\alpha=600$ keV, utilizing a coincidence technique which also accounts completely for the detector response function. The α-spectrum, containing 10^6 counts, has been incorporated into both R– and K–matrix analyses along with the previously measured ^{12}C(α,γ)^{16}O cross section and the ^{12}C+α elastic phase shifts to yield a much improved value for $S_{E1}(300)$ keV. In light of this new determination of $S_{E1}(300)$, the available radiative capture data and elastic scattering phase shifts are re-analysed, along with β-delayed α-spectrum of ^{16}N in an attempt also to place improved limits on the $S_{E1}(300)$ contribution to the ^{12}C(α,γ)^{16}O cross section.

1. Introduction

The measurement of the rate of the $^{12}C(\alpha,\gamma)^{16}O$ reaction has been the subject of numerous studies in recent years because of its importance to the helium burning process in massive stars. The extrapolation of its rate to the astrophysically important energy of E_{cm}=300 keV, however, did not result in a significant constraint on the total S-factor $S_{tot}(300)$, where the S-factor is given by $S=Ee^{2\pi\eta}\sigma$ and η is the Sommerfeldt parameter. These measurements and theoretical extrapolations of the measured radiative capture cross sections are thoroughly discussed in ref.[1] in which a first measurement of the β-delayed α-spectrum of ^{16}N is also reported. There, it has been shown that the results of this latter measurement are extremely effective in constraining the value of the E1 part of the extrapolated radiative capture cross section. Interest in these studies has been further heightened by a recent theoretical study[2] of the helium burning process where the total S-factor has been predicted to have the value $S_{tot}(300)=170\pm20\%$ keV·b. Extensive background information for the present report can be found in the two references quoted above.

In this report, two main issues are addressed. First, the experimental methods and results of the new study[1] of the β-delayed α-spectrum of ^{16}N using the TISOL[3,4] facility at TRIUMF are reviewed in §2 and §3. Second, two methods are employed to incorporate the reported $^{12}C(\alpha,\gamma)^{16}O$ results[5,6,7,8], along with the elastic scattering phase shifts[9], into the extrapolation of the measured radiative capture cross sections. The R- and K-matrix parametrizations used in these methods are reviewed briefly in §4. In the first and usual method (§5), the published values of the E1 radiative capture cross sections and the $\ell=1,2$ and 3 elastic phase shifts are used with the ^{16}N data in simultaneous R- or K-matrix fits to yield $S_{E1}(300)$. In the second and new method (§6), the ^{16}N results and the elastic scattering phase shifts are combined directly with the γ-ray angular distributions, also in simultaneous analyses, to yield both $S_{E1}(300)$ and $S_{E2}(300)$. In this second method, the intermediate step of separately fitting each $^{12}C(\alpha,\gamma)^{16}O$ angular distribution to yield the ratio[5] σ_{E2}/σ_{E1} at that specific energy was circumvented by fitting directly to the primary angular distributions themselves.

2. Experimental Considerations

For the analysis of the β-delayed α-spectrum from $^{16}N(t_{1/2}=7.1$ s) to lead to a precise determination of the reduced α-width of the $J^\pi=1^-$ sub-threshold state, the α-spectrum needs to be measured down to an energy of $E_\alpha \leq$ 600 keV. This imposes severe demands on the experiment of which the following are the most important: (i) reduction of the β-ray background because the overall α-particle yield is only 10^{-5} that of the β-yield; (ii) rejection of energy-degraded α-particles from the main α-peak since the interference peak is expected to be only 10^{-3} of the main peak; (iii) minimization of distortions to the α-spectra and the energy calibration spectra due to energy loss and straggling in the collector foils; and (iv) determination of the energy-dependent coincidence efficiency down to the lowest expected energy of the recoil ^{12}C-particles ($E_{12}<200$ keV).

The method employed was to detect the β-delayed α-particles in coincidence with their recoil ^{12}C-partners from the decay of ^{16}N atoms implanted into very thin (10 $\mu g\cdot cm^{-2}$) carbon collector foils. The thick target, on-line isotope separator TISOL[3,4] was used to produce the ^{16}N ion beam for implantation. A beam of 500 MeV protons with an intensity of up to 1.5 μA irradiated a

DISCLAIMER

thick (13 g·cm^{-2}) target of zeolite. A beam of ^{16}N ions was then extracted at 12 keV at the mass A=30 position, and implanted into the thin self-supporting carbon foils. Trace amounts of molecular beams containing ^{17}N and ^{18}N accompanied the ^{16}N beam.

The coincidence system used pairs of very thin, transmission mounted Si surface barrier detectors (10.6-15.8 μm thick). The members of each pair of coincidence detectors (Dl-D2, D3-D4, D5-D6) were placed face-to-face to take advantage of the 180 degree correlation between the particles, and their separation (8-10 mm) was such as to yield an absolute coincidence efficiency of about 30%. A wheel containing 12 implantation foils, of which only four were used at a time, was located perpendicular to the direction of the ^{16}N ion beam from TISOL. The implantation of ^{16}N-ions occurred in one of the foils. After a collection time of 3 s, the wheel was rotated through 90° in 0.25 s, successively carrying each foil from the implantation point to positions between each of the three pairs of coincidence detectors. In addition, a thick (500 μm) detector (D7) was mounted directly behind D1 to monitor the β-decay count rate during the experiment, and to detect β-delayed protons in additional calibration experiments.

The coincidence electronics and data acquisition system consisted of standard NIM and CAMAC electronics. Both singles and coincidence events were monitored on-line and stored on magnetic tape, event-by-event, for off-line analysis. Beta-decay lifetime information was obtained with the use of a clock started each time the motion of the foil wheel ceased.

3. The β-delayed α-spectrum of ^{16}N

The primary means of identifying acceptable ^{16}N α-decays was the ratio of α- to ^{12}C-pulse heights. Fig. 1 shows a 2-D spectrum of the coincident events for the D3-D4 detector pair. The α- and ^{12}C-pulse heights for a coincident event are the coordinates for each point. The system was symmetrical so that events were recorded for the α-particles detected in either detector. The intense linear diagonal bands of constant pulse height ratio are the acceptable events. The observed pulse height ratio is near 4:1 (expected 3:1) since the energy calibration is for α-particles and the ^{12}C particles undergo greater pulse height defect in the detectors and larger energy loss in both the foil and the detector entrance window. The intense horizontal and vertical bands extending towards "zero" from the main α-peaks are a result of the response function of the detector−source system. These events are cleanly separated from the acceptable coin-

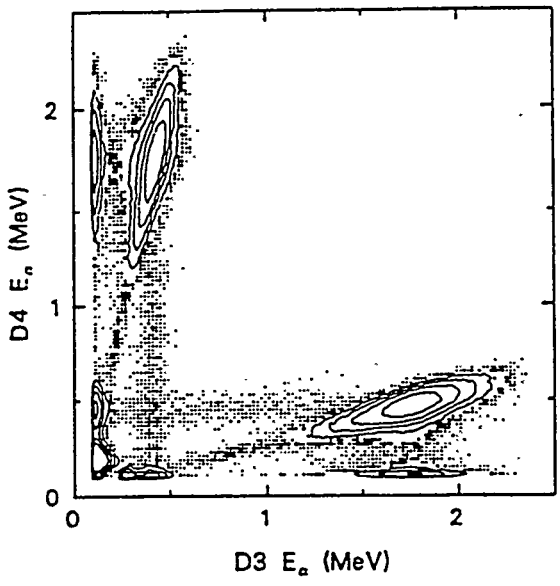

Fig. 1 Contour plot of coincidence events for D3 versus D4

cidences in the energy region of the interference peak right up to the beginning of the main α-peak. The very small number of events outside these bands constitute the random background. With the use of this selection technique, a total of 1.0265×10^6 acceptable events was obtained.

Energy calibrations of all spectra were performed frequently during the run using ^{18}N beams (mass A=34). Additional calibration experiments were performed under identical "detector/foil" conditions using a ^{20}Na beam from TISOL. Off-line calibrations with ^{148}Gd were also accomplished. Small quantities of ^{17}N and ^{18}N were present in the beam. Because of its short half-life (0.624 s), little ^{18}N is present in the spectra of D3-D6. In addition, the characteristic shape of the α-spectrum made the subtraction of 630 ± 60 events straight-forward with negligible increase in statistical uncertainty. Extensive studies of the mass-systematics of the TISOL ion beams, along with off-line γ-ray studies, established that 2500 ± 1300 counts due to ^{17}N (t=4.2 s) were present in the final 1.0265×10^6 acceptable coincidence events. The final, corrected α-spectrum from ^{16}N is shown in Fig. 2. The background events for ^{17}N and ^{18}N are also shown.

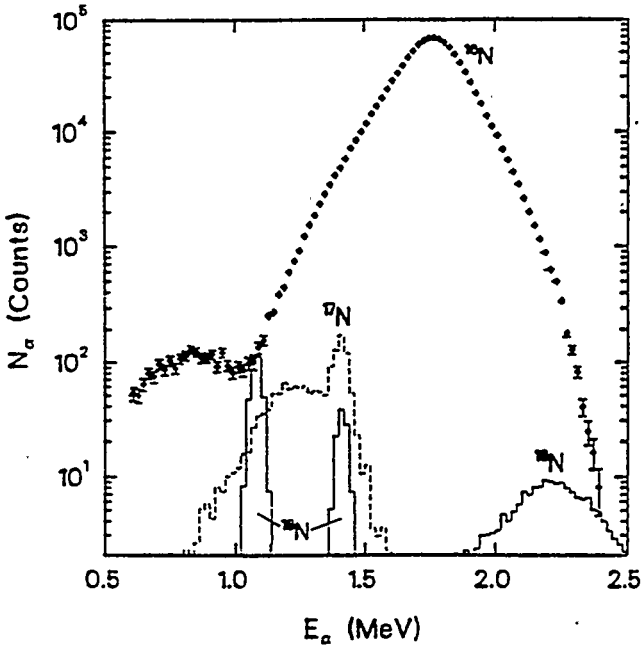

Fig. 2 Final α-spectrum from ^{16}N along with the ^{17}N and ^{18}N contributions

The energy dependence of the coincidence efficiency was determined by direct comparison of the shapes of the singles and coincidence spectra from ^{18}N. The coincidence efficiency was found to be constant to within $\pm1\%$ down to the energy of the lowest α-peak at 1.081 MeV. Below this energy, the ^{16}N coincidence events, including the entire α-response tail, were compared with the singles events. In this way the coincidence efficiency was found to be constant to $\pm6\%$ to an energy of E_α=750 keV. The efficiency was further investigated through the β-delayed proton-decay of ^{17}Ne. Each proton decay produces a corresponding ^{16}O-recoil nucleus of 1/16 of the energy of the accompanying proton. A measurement of the coincidence efficiency, similar to the above, was therefore possible to very low ion-recoil velocities (equivalent to $E_{12}<200$ keV). These results indicate that the coincidence efficiency was independent of energy to $\pm1\%$ down to E_α=1 MeV, and to $\pm6\%$ for E_α down to 550 keV.

4. R- and K-Matrix Paramametrizations and Extrapolations

In most analyses to date, R- and K-matrix analyses[1,10,11,12,13] were used to fit the experimental

results and to carry out the extrapolations. Details of these methods, as well as goodness-of-fit criteria, are given in ref.[1]. In summary, the β-delayed α-yield $W(E)$, the $^{12}C(\alpha,\gamma)^{16}O$ cross section $\sigma_{E1}(E)$, and the elastic scattering phase shifts $\delta_\ell(E)$ were fitted with a common set of R- or K-matrix parameters. These parameters were then determined jointly in a least squares fit to the experimental data with the use of the CERN minimizing routine MINUIT. In the β-decay of ^{16}N ($J^\pi=2$), excited states in ^{16}O with $J^\pi=1^-,2^-$, and 3^- are populated. The ^{16}N data can hence provide information only for the E1 component of the radiative capture. In the combined analysis of all three types of data, the following set of states were found to play a role. For $J^\pi=1^-$ and all data sets, the known states[14] at $E_x=7.117$ MeV ($E_{cm}=-0.045$ MeV) and $E_x=9.60$ ($E_{cm}=2.400$ MeV) were included along with a higher energy background state[10]. For $J^\pi=3^-$, only the sub-threshold state was populated in the β-decay, whereas two additional states at $E_x=11.60$ ($E_{cm}=4.44$) MeV and a higher energy background state, were required for the analysis of the elastic scattering phase shifts. The energy and γ-width of the 1^- sub-threshold state were taken from ref.[14] as was the energy of the 3^- sub-threshold state.

5. $\sigma_{E1}(E)$ Fits and Extrapolations

The measured ^{16}N β-delayed α-spectrum covers the range $0.787 \le E_{cm} \le 3.90$ MeV (87 data points) while the 71 data points for the four radiative capture data sets span $0.94 \le E_{cm} \le 2.98$ MeV. The $\ell=1$ and 3 phase shifts, with a total of 64 points were fitted for $E_{cm} \le 4.92$ MeV ($E_\alpha \le 6.5$). In the R-matrix analysis, a search was carried out to find the best fit values for $S_{E1}(300)$ and the radius parameter a. The minimum occurred at a=6.5 fm, and $S_{E1}(300)=78.7$ keV·b, with $\chi_{tot}^2=376.9$. Fig. 3 shows χ^2 and its components as functions of $S_{E1}(300)$. Complete details of the fitting procedure, and the final best-fit values for all the parameters are given in ref.[1] where the statistical and systematic errors are also discussed in detail. The final R-matrix result is $S_{E1}(300)=79\pm21$ keV·b, while the K-matrix gives $S_{E1}(300)=82\pm26$ keV·b. Finally, a short discussion of possible systematic errors concerning the subtraction of ^{18}N and ^{17}N contaminant events in the ^{16}N data is reported here. A combined analysis excluding all ^{16}N events in the range $1.0\ \text{MeV} \le E_\alpha \le 1.5$ MeV was performed. This circumvented entirely the issue of contaminant-subtraction. The result was $S_{E1}(300) = 84\pm21$ keV·b. Clearly, the final results are quite insensitive, within errors, to the subtraction of contaminent events at the level encountered here. It is apparent that the results are primarily dependent on both the good statistical precision in the region of the interference peak and on the detailed spectral shape over the entire α-spectrum.

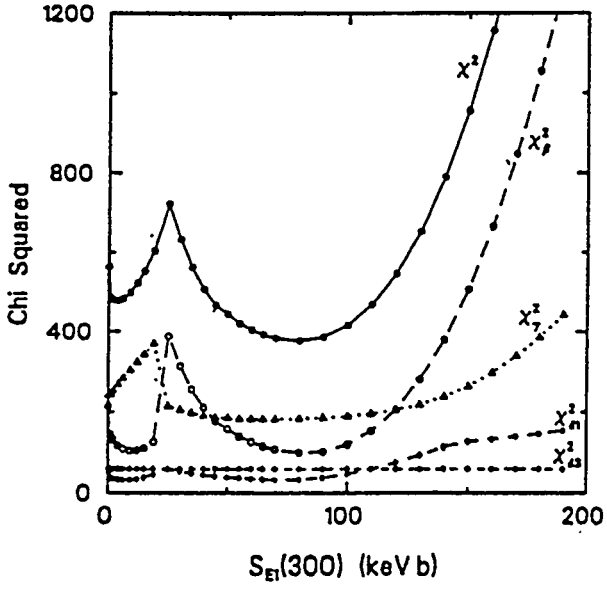

Fig. 3 Shows the total χ^2 and its components versus S_{E1}

6. Fits Directly to the (α,γ) Angular Distributions: $\sigma_{E1}(E)$ and $\sigma_{E2}(E)$

In the previous analyses of the $^{12}C(\alpha,\gamma)^{16}O$ angular distributions, each distribution at a specific energy was analysed in terms of Legendre polynomials, independently of all other distributions. These analyses were insensitive to the correlations that exist between the values and errors of the cross-sections determined at one energy and those at adjacent energies. Also it has been observed in the present work that the reduced χ^2 for the best independent fits at a specific energy were often substantially less than those determined in the method of surface fits described below, possibly reflecting the influence of systematic errors of the measurements. For these reasons a new method of analysis was developed which, together with the ^{16}N data and the elastic phase shifts, involves global fits to the surface defined by the multitude of ^{12}C $(\alpha,\gamma)^{16}O$ angular distributions at the various energies. The surface $\sigma_{\alpha\gamma}=\sigma_{\alpha\gamma}(\Theta,E)$ is analysed in terms of both the angular distribution function and the R-matrix paramaterizations (which carry the energy dependencies). Such surface fits take into account the correlations, and are particularly useful in revealing the systemic errors alluded to above. Finally, since the E1 and E2 components are treated as separate contributions in the parameterization of the $^{12}C(\alpha,\gamma)^{16}O$ angular distributions, a fit yields both $\sigma_{E1}(E)$ and $\sigma_{E2}(E)$ (while preserving the correlations between them, and possibly averaging the effects of systematic errors, which is not the case in the analysis of §5).

The γ-ray angular distributions were taken from ref.[5] (four distributions each with 10 angles), ref.[6] (three distributions each with 8 angles) and ref.[8] (16 distributions each with 6 angles). In addition, the 90° data of ref.[5] (with the E2 component explicitly included), and the total cross-section data of ref.[15] were included in the fits. The E2 cross-section was assumed to consist of contributions from the E_{cm} $(J^\pi=2^+)=-0.245$ MeV sub-threshold state, a direct capture component (DC) and a background state. The R-matrix equations for σ_{E2} were taken from ref.[13] where a complete discussion of these equations can be found.

Finally, the energy- and angle-dependent yield is given by[5]

$$W_{\alpha\gamma}(\theta,E) = 1-Q_2P_2(\theta)+\frac{\sigma_{E2}(E)}{\sigma_{E1}(E)}\left[1+\frac{5}{7}Q_2P_2(\theta)-\frac{12}{7}Q_4P_4(\theta)\right]+\frac{6}{\sqrt{5}}\left(\frac{\sigma_{E2}(E)}{\sigma_{E1}(E)}\right)^{1/2}\cos\Phi\left[Q_1P_1(\theta)-Q_3P_3(\theta)\right]$$

where Φ is the phase between the E1 and E2 components, and $P_\ell(\Theta)$ are the Legendre polynomials. The phase is taken to be $\Phi=\delta_1-\delta_2+\arctan(\eta/2)$[6], and the φ_ℓ are the angular correlation attenuation coefficients.

The results of the combined R-matrix fit are presented in Fig. 4 which shows a contour plot of χ^2 versus $S_{E1}(300)$ and $S_{E2}(300)$. For the best fit, the E1 component was found to be $S_{E1}(300)$ $=78\pm20$ keV·b consistent with §5. For the E2 component, only an upper limit of $S_{E2}(300)$ ≤ 140 keV·b can be deduced. It is also seen from the figure that the E1 and E2 components are essentially orthogonal to each other over most of the energy range of measurement, demonstrating that the previous analyses in terms of the E1 component alone remain valid. Finally, in all our varied analyses to date the extrapolated value of $S_{E1}(300)$ was constrained mainly by the reduced α-width of the sub-threshold state as determined from the ^{16}N results. The K-matrix analysis gave essentially the same results.

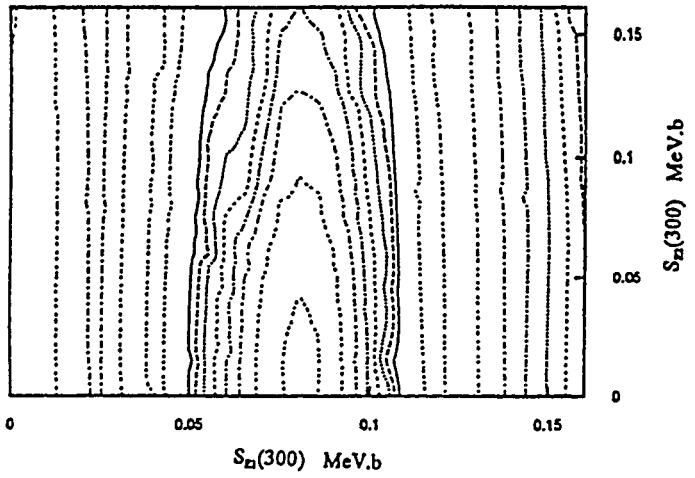

Fig. 4 Contour plot of χ^2 S_{E1} and S_{E2}

7. Conclusions

The β-delayed α-spectrum of ^{16}N has been shown to be very effective in constraining $S_{E1}(300)$. The final value is $S_{E1}(300)=79\pm21$ keV·b for the R-matrix, and 82 ± 26 keV·b for the K-matrix. A somewhat better precision is to be desired, but it is not apparent that an ^{16}N α-spectrum with improved statistics would produce the desired effect since much of the uncertainty derives from the systematic differences between the four radiative capture data sets. For the E2 component, the present results yield a tentative restriction of $S_{E2}(300)\leq 140$ keV·b. An examination of χ^2, and its components versus S_{E2} shows that the upper limit for S_{E2} is determined almost entirely by the δ_2 phase shift measurements. The present γ-ray angular correlations are ineffective in constraining the value of $S_{E2}(300)$. Measurements of γ-ray angular correlations at higher energies, where σ_{E1} and σ_{E2} are comparable are sensitive mainly to the DC-component which is very small at $E_{cm}=300$ keV. It appears that either very much improved γ-ray angular correlations at lower energies, or an independent measurement of the reduced α-width of the $J^{\pi}=2^+$ sub-threshold state are needed to constrain S_{E2}.

References

[1] R.E. Azuma, L. Buchmann, F.C. Barker, C.A. Barnes, J.M. D'Auria, M. Dombsky, U. Giesen, K.P. Jackson, J.D. King, R.G. Korteling, P. McNeely, J. Powell, G. Roy, J. Vincent, T.R. Wang, S.S.M. Wong and P.R. Wrean, Physical Rev. **C50**, 1194 (1994).

[2] T.A. Weaver and S.E. Woosley, Rhys. Rep. **227**, 65 (1993).

[3] M. Dombsky, J.M. D'Auria, L. Buchmann, H. Sprenger, J. Vincent, P. McNeely and G. Roy, Nucl. Instrum. Methods **A295**, 291 (1990).

[4] L. Buchmann, J. Vincent, H. Sprenger, M. Dombsky, J.M. D'Auria, P. McNeely and G. Roy, Nucl. Instrum. Methods **B62**, 521 (1992).

[5] P. Dyer and C.A. Barnes, Nucl. Phys. **A233**, 495 (1974).

[6] A. Redder, H.W. Becker, C. Rolfs, H.P. Trautvetter, T.R. Donoghue, T.C. Rinckel, J.W. Hammer and K. Langanke, Nucl. Phys. **A462**, 385 (1987).

[7] R.M. Kremer, C.A. Barnes, K.H. Chang, H.C. Evans, B.W. Fillippone, K.H. Hahn and L.W. Mitchell, Phys. Rev. Lett. **60**, 1475 (1988).

[8] J.M.L. Ouellet, H.C. Evans, H.W. Lee, J.R. Leslie, J.D. MacArthur, W. McLatchie, H.-B. Mak, P. Skensved, J.L. Whitton, X. Zhao and T.K. Alexander, Phys. Rev. Lett. **69**, 1896 (1992).

[9] R. Plaga, H.W. Becker, A. Redder, C. Rolfs, H.P. Trautvetter and K. Langanke, Nucl. Phys. **A465**, 291 (1987).

[10] F.C. Barker, Aus. J. Phys. **24**, 777 (1971).

[11] B.W. Fillippone, J. Humblet and K. Langanke, Phys. Rev. **C40**, 515 (1989).

[12] X. Ji, B.W. Fillippone, J. Humblet and S.E. Koonin, Phys. Rev. **C41**, 1736 (1990).

[13] F.C. Barker and T. Kajino, Aus. J. Phys. **44**, 369 (1991).

[14] F. Ajzenberg-Selove, Nucl. Phys. **A460**, 1 (1986); **A471**, 1 (1987); D.R. Tilley, H.R. Weller and C.M. Cheves, *ibid.* **A564**, 1 (1993).

[15] K.U. Kettner, H.W. Becker, L. Buchmann, J. Görres, H. Kräwinkel, C. Rolfs, P. Schmalbrock, H.P. Trautvetter and A. Vlieks, Z. Phys. **A308**, 73 (1982).